Development of a new generation of miniemulsion based on cottonseed oil with α-tocopherol and ZnO and evaluation of its adjuvant activity

Gustavo Sobrevilla-Hernández [1] , Moisés Armides Franco-Molina [Corresp., 1] , Diana G. Zárate-Triviño [1] , Jorge R. Kawas [2] , Sara Paola Hernández-Martínez [3] , Paola Leonor García-Coronado [1] , Silvia Elena Santana-Krymskaya [1] , Cynthia Aracely Alvizo-Báez [1] , Cristina Rodríguez-Padilla [1]

[1] Laboratorio de Inmunología y Virología, Facultad de Ciencias Biológicas, Universidad Autónoma de Nuevo León, San Nicolás de los Garza, Nuevo León, Mexico

[2] Posgrado Conjunto Agronomía-Veterinaría, Universidad Autónoma de Nuevo León, General Escobedo, Nuevo León, Mexico

[3] Facultad de Agronomía, Universidad Autónoma de Nuevo León, General Escobedo, Nuevo León, Mexico

Corresponding Author: Moisés Armides Franco-Molina
Email address: moyfranco@gmail.com

Background Emulsions have been widely used as immunological adjuvants. But the use of materials derived from plants such as cottonseed oil, alpha-tocopherol, or minerals such as zinc, as well as their use at the nanometric scale has been little explored. In this study, we develop a new miniemulsion and evaluated its antioxidant and phagocytic capacity, as well as parameters related to immune response stimulation by cytokine expression and antibodies production in a mice model. **Methods** Formulated CN (cottonseed oil miniemulsion) and CNZ (Cottonseed oil miniemulsion whit zinc oxide nanoparticles) miniemulsions were characterized by scanning electronic microscopy SEM, DLS and FT-IR. In murine macrophages, splenocytes and thymocytes primary cultures safety and cytotoxicity were determined by MTT. In macrophages the antioxidant and phagocytic capacity was evaluated. In BALB/c mice, the stimulation of the immune system was determined by the expression of cytokines and the production of antibodies. **Results** The CN and CNZ presented stability for 90 days. Immediately after preparation, the CN presented a higher particle size (543.1 nm) than CNZ (320 nm). FT-IR demonstrated the correct nanoparticle synthesis by the absence of sulfate groups. CN and CNZ (1.25 to 10 µL/mL) had no toxic effect on macrophages (p=0.108), splenocytes (p= 0.413), and thymocytes (p= 0.923). All CN and CNZ doses tested induced nitric oxide and antioxidants production in dose dependent manner when compared with control. CN-ovalbumin and CNZ-ovalbumin treatments in femoral subcutaneous tissue area showed inflammation with higher leukocyte infiltration compared with FCA. The intraperitoneal administration with CN, CNZ, and FCA showed a higher total intraperitoneal cells recruitment (CD14$^+$) after 24 h of inoculation than control (p=0.0001). CN and CNZ increased the phagocyte capacity

with respect to untreated macrophages in the *Candida albicans*-phagocytosis assay. The evaluation of residual CFU indicated that only CN significantly decreased (p=0.004) this value at 3 h. By other side, only CN increased (p=0.002) the nitric oxide production. CNZ stimulated a major INFγ secretion compared with FCA at day 7. A major IL-2 secretion was observed at days 7 and 14, stimulated with CN and CNZ. Both miniemulsions did not affect the antibody isotypes production (IgG1, IgG2a, IgG3, IgA and IgM) at days 7, 14, 28, and 42. CN induced a significant IgG production against OVA, but lesser than FCA.

Conclusions The two new miniemulsions with adjuvant and antioxidant capacity, were capable of generating leukocyte infiltration and increased cytokines and antibodies production.

1 **Development of a new generation of miniemulsion based on**

2 **cottonseed oil with α-tocopherol and ZnO and evaluation of its**

3 **adjuvant activity.**

5 Gustavo Sobrevilla-Hernández [1], Moisés Armides Franco-Molina [1*], Diana G. Zárate-Triviño [1],

6 Jorge R. Kawas [2], Sara Paola Hernández-Martínez [3], Paola Leonor García-Coronado [1], Silvia

7 Elena Santana-Krymskaya [1], Cynthia Aracely Alvizo-Báez[1], Cristina Rodríguez-Padilla[1]

9 [1] Facultad de Ciencias Biológicas, Laboratorio de Inmunología y Virología, Universidad

10 Autónoma de Nuevo León, San Nicolás de los Garza, Nuevo León, México.

11 [2] Posgrado Conjunto Agronomía-Veterinaria, Universidad Autónoma de Nuevo León, Escobedo,

12 NL, Mexico.

13 [3] Facultad de Agronomía, Av. Universidad Autónoma de Nuevo León, General Escobedo, Nuevo

14 León, México.

18 *Corresponding Author:

19 Moisés A. Franco-Molina[1]

20 Av. Universidad s/n, Cd. Universitaria, San Nicolás de los Garza, Nuevo León, C.P. 66451,

21 México.

22 Email address: moyfranco@gmail.com

24 **Abstract**

26 **Background**

27 Emulsions have been widely used as immunological adjuvants. But the use of materials derived

28 from plants such as cottonseed oil, alpha-tocopherol, or minerals such as zinc, as well as their use

29 at the nanometric scale has been little explored. In this study, we develop a new miniemulsion and

30 evaluated its antioxidant and phagocytic capacity, as well as parameters related to immune

31 response stimulation by cytokine expression and antibodies production in a mice model.

32 **Methods**

33 Formulated CN (cottonseed oil miniemulsion) and CNZ (Cottonseed oil miniemulsion whit zinc

34 oxide nanoparticles) miniemulsions were characterized by scanning electronic microscopy SEM,

35 DLS and FT-IR. In murine macrophages, splenocytes and thymocytes primary cultures safety and

36 cytotoxicity were determined by MTT. In macrophages the antioxidant and phagocytic capacity

37 was evaluated. In BALB/c mice, the stimulation of the immune system was determined by the

38 expression of cytokines and the production of antibodies.

39 **Results**

40 The CN and CNZ presented stability for 90 days. Immediately after preparation, the CN presented

41 a higher particle size (543.1 nm) than CNZ (320 nm). FT-IR demonstrated the correct nanoparticle

42 synthesis by the absence of sulfate groups. CN and CNZ (1.25 to 10 µL/mL) had no toxic effect

43 on macrophages (p=0.108), splenocytes (p= 0.413), and thymocytes (p= 0.923). All CN and CNZ

44 doses tested induced nitric oxide and antioxidants production in dose dependent manner when

45 compared with control. CN-ovalbumin and CNZ-ovalbumin treatments in femoral subcutaneous

46 tissue area showed inflammation with higher leukocyte infiltration compared with FCA. The

47 intraperitoneal administration with CN, CNZ, and FCA showed a higher total intraperitoneal cells

48 recruitment (CD14$^+$) after 24 h of inoculation than control (p=0.0001). CN and CNZ increased the

49 phagocyte capacity with respect to untreated macrophages in the *Candida albicans*-phagocytosis

50 assay. The evaluation of residual CFU indicated that only CN significantly decreased (p=0.004)

51 this value at 3 h. By other side, only CN increased (p=0.002) the nitric oxide production. CNZ

52 stimulated a major INFγ secretion compared with FCA at day 7. A major IL-2 secretion was

53 observed at days 7 and 14, stimulated with CN and CNZ. Both miniemulsions did not affect the

54 antibody isotypes production (IgG1, IgG2a, IgG3, IgA and IgM) at days 7, 14, 28, and 42. CN

55 induced a significant IgG production against OVA, but lesser than FCA.

56 **Conclusions**

57 The two new miniemulsions with adjuvant and antioxidant capacity, were capable of generating

58 leukocyte infiltration and increased cytokines and antibodies production.

59

60 **Introduction**

61   Adjuvants have been used to increase the antigens immunogenicity in vaccines or to modulate the

62   immune system in diverse conditions of disease. Adjuvants can be obtained from plants, bacterial

63   products, complex carbohydrates, animal extracts, and synthetic cytokines (Shahbazi and

64   Bolhassani, 2016). Emulsion adjuvants employing mineral oils have an extensive clinical history

65   use dating back to the 1930s (Shah *et al.,* 2015). Different emulsion types have been used as

66   immunostimulants or adjuvants in therapeutic or prophylactic vaccination, emulsions are formed

67   when two immiscible liquids are brought together and one of them is organized into small droplets

68   dispersed within the other, and stabilized by an interfacial surfactant layer. Emulsions can be

69   formulated either as water-in-oil (W/O), oil-in-water (O/W) or water-in-oil-in-water (W/O/W)

70   (Burakova *et al.,* 2018). However, emulsions in some occasions can induce strong adverse

71   reactions, such as local inflammatory lesions, pain, and distress, reason why, their use has been

72   prohibited in animal and human vaccines (Burakova *et al.,* 2018). Hence biocompatible oil-in-

73   water emulsions based on vegetable or animal oils have been explored in efforts to improve

74   tolerability, by decreasing the amount of oil and improving their biodegradability (Shah *et al.,*

75   2015).

76   Squalene is a type of unsaponifiable lipid that acts as a biosynthetic precursor to all steroids in

77   plants and animals (He and Corke, 2003). Some emulsions developed as adjuvants were based in

78   squalene. Squalene-based adjuvants have been administered to humans, including children, and a

79   good safety profile has been established. Given the public's perception regarding to squalene

80   safety, and misunderstandings regarding to its source, it is necessary to determine whether any

81   other oil could be used as replacements for squalene (Fox *et al.,* 2011). Vegetable oils can be used

82   as an alternative adjuvant to squalene-based emulsions in vaccines and immunostimulants, because

83   of their long variety of active substances that can affect the immune system. Several vegetable oils

84   have α-tocopherol, (Grilo *et al*., 2014). This one has immunomodulatory effect on dendritic cells

85   (DCs), macrophages, natural killer (NK) cells, T cells, and B cells development, function and

86   regulation (Lee and Han, 2018). Cottonseed oil contains α-tocopherol (411±8.23 to 470.0±9.4

87   mg/kg) (El-Mallah et al., 2011); AS03 commercial emulsion used as adjuvant in Prepandrix (pre-

88   pandemic H5N1) and Pandemrix (pandemic H1N1) influenza vaccines contain α-tocopherol as

89   immune potentiator (Shah *et al.,* 2015). Otherwise, zinc is a nutritional mineral that participates in

90   a variety of cellular functions, including signal transduction, transcription, and replication;

91   strongly influencing the immune system affecting both nonspecific and acquired immunity

92   (Dardenne, 2002). However, zinc oxide (ZnO) in nanoparticle form has not been used before as

93   part of an immunogenic adjuvant. We aimed to develop a new miniemulsion and study its

94   antioxidant and phagocytic capacity as well as parameters related to immune response stimulation

95   by expression of cytokine and antibodies production in a mice model.

96

Materials & Methods

Minioemulsion development and characterization

Reactive

100   All reactive were used without additional purification, cottonseed oil pharmaceutical grade, α-

101   tocopherol (96% purity), zinc sulfate monohydrate ($ZnSO_4 \cdot H_2O$), sodium hydroxide (NaOH),

102   Tween 20, and DMSO (Dimethyl sulfoxide) were purchased from Sigma-Aldrich Inc (Saint Louis,

103   USA). Fetal bovine serum (FBS) (ThermoFisher Scientific, USA), DMEM culture medium

104   (ThermoFisher Scientific, USA), 3-(4,5-dimethylthiazol-2-yl-2,5-diphenyltetrazol) bromide

105   (MTT) (ThermoFisher Scientific, USA), the Antioxidant assay kit (Catalog No. KA1622, Abnova,

106   Taipei, Taiwan), Griess reaction (Griess Reagent, Catalog No. ab234044, Abcam, Cambridge,

107   UK) , Lipopolysaccharide (Sigma-Aldrich Inc Saint Louis, USA), Neutral Red Assay Kit-Cell

108   Viability / Cytotoxicity (Catalog No. ab234039, abcam, Cambridge, UK), Phagocytosis assay kit

109   (IgG FITC) (Catalog No. 500290 Cayman chemical, MI, USA), *C. albicans* (ATCC 10261).

110   Ovalbumin (OVA), (Sigma-Aldrich Inc Saint Louis, USA), Freund′s Adjuvant Complete (FCA),

111   (Sigma-Aldrich Inc Saint Louis, USA). Ig Isotyping Mouse Uncoated ELISA kit (Catalog No. 88-

112   50630, Thermo Fisher Scientific Inc, Viena, Austria). Mouse Th1/Th2/Th17 Cytokine kit (Catalog

113   No. 560485, DB biosciences, San Jose, Ca, US). Formaldehyde (Catalog No. F8775 Sigma-

114   Aldrich Inc., Saint Louis, USA). Hematoxylin and eosin (H&E) (Catalog No. ab245880, Abcam,

115   Cambridge, UK), CD14 Monoclonal Antibody (Sa2-8), APC, eBioscience(Catalog No.17-

116   0141-82, Thermo Fisher Scientific Inc, Viena, Austria).

117   **Zinc oxide nanoparticles synthesis**

118   The Zinc oxide (ZnO) nanoparticles were obtained by the coprecipitation method. Zinc

119   sulfate monohydrate ($ZnSO_4 \cdot H_2O$) was dissolved in deionized water at 0.5 M that remained

120   under stirring at 300 rpm while sodium hydroxide solution (2 M NaOH) was added in drops.

121 After, the supernatant was discarded, and the precipitate formed was washed with deionized

122 water and centrifuged at 8,000 rpm for 10 min. Precipitate was dried in a hot air oven at 60

123 °C for 24 h. Then, the obtained powder was calcinated at 300 °C for 2 h, in a muffle.

124 **Miniemulsion formulation**

125 Two miniemulsions were produced as follow: 1) Cottonseed oil miniemulsion (CN) (to form

126 the oil phase of 275 mg), in which α -tocopherol (25 mg), Tween 20 (35 mg) and DMSO (50

127 ml) were dissolved, and 2) cottonseed oil miniemulsion + ZnO nanoparticles (CNZ) was

128 formulated in the same way as described above plus the addition of ZnO nanoparticles (2.5

129 µg) in the oil phase. The oil phase was calibrated with saline solution (1 mL) and mixed at

130 12,000 rpm in homogenizer for 10 min. (ULTRA-TURRAX®, IKA Works Inc, Wilmington,

131 US).

132 **Miniemulsion characterization**

133 Droplet size and polydispersity index (PDI) were determined by dynamic light scattering (DLS)

134 and Zeta potential (PZ) was determined by electrophoretic mobility measurements in a ZS90-Nano

135 Zetasizer (Malvern Instruments). All results were measured in triplicate at room temperature (25

136 °C). The ZnO nanoparticles were characterized by X-ray diffraction (XRD) and the Fourier

137 Transform Infrared Spectroscopy (FT-IR), ZnO nanoparticles morphology and size were

138 confirmed by scanning electron microscopy (SEM), and the droplet size was confirmed by atomic

139 force microscopy (AFM), images were analyzed with Gwyddion software. The characterization of

140 miniemulsions functional groups and their components (cottonseed oil, α-tocopherol, and ZnO

141 nanoparticles) were determinate by attenuated total reflection (ATR) in conjunction with FT-IR

142 technique. The samples were placed onto the diamond ATR crystal, and spectra was recorded by

143 a FT-IR (PERKIN ELMER, Waltam, MA, USA), with an accumulation of 16 scans at a resolution

144 of 4 cm^{-1} between 4500-500 cm^{-1}. Data were analyzed with the software PERKIN ELMER

145 spectrum 10.

146 **Animals**

147 Male BALB/c mice (6–8 weeks old, weighing 23±2g) were used for all *in vivo* and *ex vivo*

148 experiments. The animals were obtained from the Bioterium of Facultad de Ciencias Biológicas

149   of the Universidad Autónoma de Nuevo León, (UANL, FCB) under the approval of Bioethics

150   committee protocol No. CEIBA-2019-015. Animals were housed 8 per cage (polypropylene) under

151   constant specific conditions with temperature at 24 °C, 50% relative humidity and a controlled

152   light and dark cycle (12h: 12h) with ventilated caging systems, wood sawdust bedding and

153   standardized environmental enrichment. Feed (pellet total mix ration) and clean water were

154   supplied *ad libitum*. For sample (serum, macrophage, thymocyte and splenocyte) collection,

155   animals were euthanized by overdoses of anesthesia (ketamine-xylazine protocol).

156   **Cell obtention and culture conditions**

157   Thymus, spleen, and peritoneal macrophages primary cultures were obtained from healthy mice.

158   Cell cultures were maintained in a medium containing 5% fetal bovine serum (FBS), antibiotic

159   and antimycotic 1%, under an atmosphere of 5% CO_2 and 95% air at a constant temperature of 37

160   °C.

161   **Ethical statement**

162   All the experiments pertaining to animal use and their care strictly followed the guidelines of the

163   Official Mexican Standard (NOM-062-ZOO-1999) on technical specifications for production, care

164   and use of laboratory animals. All the protocols were approved by UANL FCB Animals Ethics

165   Committee (protocol CEIBA-2019-015).

166   **Cell toxicity**

167   The miniemulsions toxicity was evaluated *in vitro* in thymus, spleen, and peritoneal macrophages

168   primary cultures. Cells were seeded in 96-well plates at a density of 2×10^5 cells/well with 100 µL

169   of DMEM culture medium. After 24 h of incubation culture medium was replaced by new one

170   containing CN or CNZ (0, 1.25, 2.5, 5 and 10 µL/ml). Cell viability was evaluated 24 h after

171   treatment using the technique of MTT. The spectrophotometry measurement was performed in

172   triplicate at 570 nm in a plate reader (Synergy HT, Biotec), the percentage of viability was

173   determined by the following equation:

174   Viability (%) = (Absorbance of the sample / Absorbance of the control) * 100

175   **Macrophage NO (nitric oxide) and antioxidants production**

176 For the miniemulsions effect over nitric oxide production (as nitrite) and total antioxidant capacity
177 (TAC), murine peritoneal macrophages (MPM) were used. As positive control lipopolysaccharide
178 (LPS) was used in a concertation of 5 µL/ mL (Sigma-Aldrich Inc Saint Louis, USA).

179 Nitrite concentration in treated cells supernatant was determined by Griess reaction (Griess
180 Reagent, Catalog No. ab234044, Abcam, Cambridge, UK). MPM were cultured in the same way
181 as mentioned in the cell toxicity assays section described above. Supernatants (50 µL) were
182 collected, centrifuged at 600×g for 5 min, mixed with 100 µL of Griess reagent [0.1% N-(1-
183 naphthyl)-ethylene diamine, 1% sulfanilamide in 5% phosphoric acid] and incubated at room
184 temperature for 10 min. Absorbance was measured at 540 nm (Bie et al., 2019).

185 TAC was determinate in MPM culture supernatants. MPM were cultured and supernatants were
186 collected under conditions described above. The Antioxidant assay kit (, Catalog No. KA1622,
187 Abnova, Taipei, Taiwan) was used according to manufacturer's instructions. Assay measures TAC
188 by the reduction of Cu^{+2} to Cu^{+} observed by a colored complex formation. Trolox (6-hydroxyl-
189 2,5,7,8-tetra methyl chroman -2- carboxylic) standard curve was measured at 540 nm.

190 **Macrophage uptake and phagocytosis**

191 Two assays were designed to determine the miniemulsions uptake and phagocytic activity effect
192 in MPM. CN and CNZ (10µL/mL) were used as cell stimulation treatment, for phagocytosis
193 inhibition control disodium clodronate (0.6 mg/ mL) was used and DMEM medium as negative
194 control. MPM quantitative uptake capacity was determinate by neutral red assay (Bie et al., 2019)
195 using Neutral Red Assay Kit - Cell Viability / Cytotoxicity (Catalog No. ab234039, abcam,
196 Cambridge, UK) according to manufacturer's instructions. For the assay, 2 x 10^5 murine peritoneal
197 macrophages were seeded on 96-well plates, washed 3 times with PBS, and then incubated with
198 10% neutral red for 2 h. After 3 washes, neutral red incorporated into lysosomes was dissolved by
199 the lysis solution provided by the kit, and the absorbance was read at 540 nm. Qualitative
200 phagocytic activity was determined using Phagocytosis assay kit (IgG FITC) (Catalog No. 500290
201 Cayman chemical, MI, USA). MPM were seeded on coverslips in 6-well plates and incubated for
202 24 h in DMEM medium. After 1h of treatments cells were incubated with latex beads-rabbit IgG-
203 FITC complex for 2 h. Photographies were observed in fluorescence microscope (Axioscope 5
204 Pol, Zeiss, Oberkochen, Germany).

205 *Candida Albicans* **macrophages phagocytosis**

206 For the evaluation of the MPM phagocytic capacity, *C. albicans* (ATCC 10261) was used. MPM,

207 obtained from three healthy mice were seeded under the previously described conditions in the

208 cell toxicity assay. Phagocytosis assay was performed based in the method proposed by Alieke et

209 al (2002). Co-culture supernatant (macrophages ($1X10^6$ cells) / *C. albicans* ($1X10^6$-$1X10^8$ cells)

210 proportion) was collected to assess the increase or decrease of colony forming units (CFU) by the

211 Mc-Farland method (César-de Vasconcelos et al., 2014). The percentage of phagocytized

212 microorganisms was defined as following equation:

213 (1- (Number of un-phagocyted CFU/CFU at the start of incubation)) *100.

214 Death of *C. albicans* by phagocytes was assessed in the same monolayers. The nitic oxide (as

215 nitrite) production was also determined as mentioned previously.

216 **Immunization and sample collection**

217 Three independent experiments were designed. Ovalbumin (OVA), Sigma-Aldrich Inc Saint

218 Louis, USA) was used as antigen (10 mg per animal in 50 µL of saline solution). All immunizations

219 were subcutaneously applied (s.c.) in a total volume of 100 µL per animal (50 µL of miniemulsion

220 and 50 µL of antigen). Freund′s Adjuvant Complete (FCA, Sigma-Aldrich Inc Saint Louis, USA)

221 was used as positive control; a group of only antigens was used as control (ovalbumin 10 mg per

222 dose in 100 µL of saline solution)

223 Experiment A. Mice inoculated with CN, CNZ, FCA and control were sacrificed by cervical

224 dislocation at 24 h post-treatment. The administration site (subcutaneous tissue over the femoral

225 area) was fixed in 10% formaldehyde solution and after that, covered with hematoxylin and eosin

226 (H&E) to determine leukocyte infiltration. For the quantification and cell typing, mice were treated

227 intraperitoneally with miniemulsions without antigen. The cells (cells/µL) were located by size

228 and granularity to stablish the gate, and the $CD14^+$ expression was determined by flow cytometry.

229 These assays were carried out by flow cytometry (Accuri C6, DB biosciences, San Jose, Ca, US).

230 Experiment B. Mice were immunized with OVA, and its combination with CN, CNZ, and FCA or

231 control (saline solution) on days 0 and 14. Blood samples were taken on days 7, 14, 28, and 42.

232 The blood samples were obtained from cardiac punction in anesthetized mice. Blood serum was

233 separated and frozen at -80 °C until the time of isotype antibody determination (IgG1, IgG2a,

234 IgG2b, IgG3, IgA and IgM) and determination of cytokine profile TH1 (IFN-γ, IL-2 and TNF-

235 α)/TH2 (IL-4, IL-6 and IL-10)/TH17 (IL 71a). Cytokines were measured by flow cytometry

236 (Accuri C6, DB biosciences, San Jose, Ca, US). using a commercial Cytometric Bead Array (CBA)

237 Mouse Th1/Th2/Th17 Cytokine kit (Catalog No. 560485, DB biosciences, San Jose, Ca, US).

238 Experiment C. Mice were immunized at days 0 and 14 with the different miniemulsions (CN or

239 CNZ) previously mentioned and challenged with OVA at day 42 and, blood samples were taken

240 at 72h after. The blood serum was separated to evaluate specific antibodies and frozen at -80 °C

241 until analysis.

242 **ELISA assay**

243 Anti-ovalbumin antibodies were evaluated by ELISA, as previously described (Thommen, Moleta

244 Colodel & Albuquerque, 2011). Briefly, polystyrene 96 well- plates (Falcon) were coated

245 overnight at 4 °C with 0.5 mg of OVA per well in carbonate-bicarbonate buffer pH 9.6, after that

246 washed with PBS 0.05%-Tween-20, and then blocked with 1%-BSA/PBS for 1h at room

247 temperature. Mouse antiserum from day 45 was added by triplicate (serial dilutions from 1:100)

248 and incubated overnight at 4 °C. Plates were washed and incubated for 1 h at 37 °C with goat anti-

249 mouse IgG-HRP (Catalog No. sc-2005, Santa Cruz Biotechnology Inc., Dallas, Tx). After that

250 wells were washed, and tetramethylbenzidine (TMB) was added. The reaction was stopped with

251 H_2SO_4. Plate was read at 450 nm in a plate reader (Synergy HT, Biotec), values indicating optical

252 density (DO). The antibodies isotypes (IgG1, IgG2a, IgG2b, IgG3, IgA and IgM) were determinate

253 by commercial kit Ig Isotyping Mouse Uncoated ELISA (Catalog No. 88-50630, Thermo Fisher

254 Scientific Inc, Viena, Austria).

255

256 **Statistical analysis**

257 All data analysis was performed with Minitab® (2014) software. Data was expressed as the mean

258 ± standard error (SE). For the variables of nitric oxide production and antioxidant capacity, a

259 Pearson correlation test was performed. Statistical significance (α= 0.05) was determined by

260 ANOVA. The comparison of means was performed by Tukey test.

261

262 **Results**

263 **Miniemulsion development and characterization**

264 The miniemulsion CN and CNZ presented stability for 90 days, and this was confirmed by DLS

265 analysis (Table 1 and Figure 1A and 1B). Immediately after preparation, the CN miniemulsion

266 presented a higher particle size (543.1 nm) with a zeta potential =-26.6 mV and PDI = 0.074, in

267 contrast to CNZ that presented a size of 320 nm, a zeta potential = -28.1 mV and PDI = 0.449.

268 However, after 90 days slightly differences were observed, the CN emulsion presented a decrease

269 in zeta potential (-13 mV) and increase of PDI (0.225), and CNZ presented a decrease in size

270 (259.4 nm) and PDI (0.312) but increase of zeta potential (-29.5 mV). The particle size difference

271 of CN and CNZ was confirmed by atomic force microscopy (AFM) (Figure 1c), where CN showed

272 big semispherical structures and CNZ small spherical structures.

273 The FT-IR spectra of $ZnSO_4 \cdot H_2O$ and ZnO nanoparticles is shown in Figure 2a and 2b,

274 respectively. In Figure 2a, can be observed the characteristic peaks of $ZnSO_4 \cdot H_2O$, a hydroxyl

275 group (OH) at 3,135 cm^{-1}, a carbonyl group (C=O) at 1,506 cm^{-1}, and sulfate groups (SO^{-2}_4)

276 at 1,090 y 855 cm^{-1}. The spectra of ZnO nanoparticles (Figure 2b) showed a peak at 576 cm^{-1},

277 characteristic of the ZnO stretching mode. Figure 2c indicates the principal groups of $ZnSO_4$

278 $\cdot H_2O$ and ZnO nanoparticles observed in FT-IR spectra**.** The photography by scanning electron

279 microscopy (SEM) (Figure 2c) showed agglomerates of ZnO nanoparticles with spherical

280 morphology.

281 There is a qualitative difference between two samples in the size of the emulsions, considering that

282 in Figure 1 the emulsions are larger compared to Figure 2, in addition a homogeneous size is

283 observed in the case of the emulsions with CNZ, evidence of a large amount of residues in the first

284 sample probably due to the inefficiency of the synthesis system, which indicates that in CNZ there

285 is an improvement in the synthesis by adding zinc nanoparticles, probably due to its hydrophilic

286 characteristics.

287 The Figure 3 showed the FT-IR spectra of miniemulsions and their precursors. In cottonseed oil

288 (Figure 3a) was observed the C-H group strongly stretched at 2,922 cm^{-1} and 1,465 cm^{-1};

289 stretching vibrations of carboxyl group (COOH) at 2,856 cm^{-1}, ketone group (C=O) at 1744

290 cm-1, and C-O group at 1,156 cm^{-1}. The spectra of α-tocopherol (Figure 3b) showed peaks at

291 2927 cm^{-1} and 2867 cm^{-1} that correspond to the asymmetric and symmetric stretching

292 vibrations of CH_2 and CH_3, respectively. Peak were observed at 1758 cm^{-1} for an alkene

293   group (C=C), at 1461 cm^{-1} for an asymmetric bending of a phenyl group (C$_6$H$_5$), and methyl

294   and methylene symmetric bending peaks at 1365 cm^{-1} and 1203 cm^{-1}, respectively.

295   The miniemulsion CN FT-IR spectra showed interaction of functional groups COOH, C=O

296   and C-O of cottonseed oil with the C=C and C$_6$H$_5$ functional groups of α-tocopherol (Figure 3c)

297   in addition to the interaction of ZnO nanoparticles in CNZ miniemulsion (Figure 3d).

298   Figure 3e represent the FT-IR spectra comparative of miniemulsions CN, CNZ, and

299   cottonseed oil, and Table 2 showed the principal functional groups of precursors.

300   **Effect of miniemulsions on immune cell function**

301   CN and CNZ miniemulsions at concentrations of 1.25 to 10 µL/mL had no effect on the viability

302   of macrophages (p=0.108), splenocytes (p= 0.413), and thymocytes (p= 0.923) *in vitro* (Figure 4).

303   All doses tested of CN and CNZ induced nitric oxide production in dose dependent manner when

304   compared with the control (0 µL). The CN induced a similar production of nitric oxide at doses of

305   1.25 (p= 0.998) and 2.5 (p= 0.112) µL/mL and highest at doses of 5 and 10 µL/mL (p= 0.0001)

306   when compared with the positive control (LPS). No difference (p=0.935) in nitric oxide production

307   was found at all doses tested of CNZ when compared with LPS (Figure 5).

308   **The antioxidant capacity**

309   All CN and CNZ doses tested had the capacity to induce the production of antioxidants by dose

310   dependent manner when compared with the control (p= 0.0001). The CN 5-10 µL/mL doses

311   induced a major antioxidant production (p=0.0001) than LPS and 2.5 µL/mL (p=0.979) / 1.25

312   µL/mL (p=1.0) doses induced similar productions levels. The CNZ treatment at 10 µL/mL

313   (p=0.002) dose induced a higher antioxidant total production than LPS, but at minor doses 5

314   µL/mL (p= 0.115),2.5 µL/mL (p=0.925) and 1.25 µL/mL (p= 1.0) no difference was found (Figure

315   6). There is a strong correlation between the production of nitric oxide and antioxidants in

316   macrophages treated with CN (r= 0.905, p= 0.0001) as in those treated with CNZ (r= 0.804, p=

317   0.002).

318   **Histological evaluation**

319   The histological evaluation of the tissue at the inoculation site (subcutaneous tissue on femoral

320   area) with CN or CNZ with ovalbumin showed inflammation with higher leukocyte infiltration

321   compared with CFA (Figure 7). The intraperitoneal inoculation with CN, CNZ miniemulsion and

322   CFA showed a high recruitment of total intraperitoneal cells with the CD14$^+$ phenotype, after 24

323 h of inoculation compared with control (p=0.0001), however no difference was found between

324 CN, CNZ and FCA (Figure 8).

325 **Macrophage uptake and phagocytosis**

326 The CN (p= 0.158) and CNZ (p= 0.495) miniemulsions evaluated by neutral red assay did not

327 affect the macrophages uptake activity when compared with untreated macrophages (Figure 9).

328 However, in the macrophages *Candida albicans*-phagocytosis assay the CN and CNZ

329 miniemulsions increased the phagocyte capacity with respect to the untreated macrophages (Figure

330 10). Next, the evaluation of residual colony forming units indicated that only CN significantly

331 decreased (p= 0.004) this value respect CNZ, but at 4 h no difference was found with respect to

332 the untreated macrophages (Figure 11a). By other side, only CN miniemulsion increased (p=0.002)

333 the nitric oxide production in all times evaluated (Figure 11b).

334 **Cytokine production**

335 The CNZ miniemulsion stimulated a major INFγ secretion compared with FCA at day 7

336 (p=0.0001), this difference was not observed at day 14 (p=1.0) (Figure 12). A major secretion of

337 IL-2 was observed at days 7 (p=0.027) and 14 (p=0.007), stimulated with the CN and CNZ

338 miniemulsions (Figure 12). However, the IL-10 was not affected (Figure 12).

339 **Switching Isotype evaluation**

340 The CN and CNZ miniemulsions did not affect the production of IgG1. However, the FCA

341 stimulated a major production of IgG1 at day 42 compared with the untreated mice (p=0.044)

342 (Figure 13). The CN and CNZ miniemulsions did not affect the production of IgG2b at all times

343 evaluated, only significant difference (p= 0.044) was found with FCA at day 28 (Figure 13). At

344 the last, the miniemulsions did not affect the production of antibody isotypes (IgG1, IgG2a, IgG3,

345 IgA and IgM) at days 7, 14, 28 and 42.

346 **IgG specific OVA**

347 The CN miniemulsion induced a significant production of IgG against OVA, but lesser than FCA.

348 CNZ miniemulsion did not affect this, when compared with the OVA treatment (p= 0.0001)

349 (Figure 14).

350

351 **Discussion**

352 The droplet size obtained from CN (543.1 nm) and CNZ (320 nm) formulations, the zeta potential

353 (-26.6 mV for CN and -28.1 mV for CNZ) and PDI values (0.074 for CN and 0.449 for CNZ)

354 indicate a monodisperse emulsion with a greater molecule repulsive strength which increases its

355 stability (Malik, Ameta, & Singh, 2016).

356 The results of FT-IR spectra confirmed the synthesis of ZnO nanoparticles with a peak at 576 cm^{-1},

357 characteristic of the ZnO stretching mode (Del Buono et al., 2022; Nagaraju et al., 2017), and the

358 images by SEM showed agglomerates with a spherical morphology (Vasile et al., 2015; Shah et

359 al., 2016). Similarly, FT-IR spectra confirmed the nature of cottonseed oil precursors (carboxyl

360 at 2,856 cm^{-1}, and ketone at 1744 cm^{-1}) (Bajaj, Tekade & Manoja, 2015), and α-tocopherol

361 (alkene at 1758 cm^{-1}, phenyl at 1461 cm^{-1}, methyl at 1365 cm^{-1}, and methylene at 1203 cm^{-1}

362 groups) (Lucarini et al., 2020).

363 The charges detected by Z potential measurements can be attributed to the unsaturated fatty acids

364 group of cottonseed oil, these molecules have a negative charge (El-Mallah et al., 2011; Shah et

365 al., 2017). In fact, Tween 20 is a non-ionic surfactant, but is part of the emulsion, the charge

366 depends on the interaction of phases (Xin et al, 2013).

367 The miniemulsion with ZnO nanoparticles showed more stability (ζ potential values CN =-13 mV

368 CNZ =-29.5mV at 3 months) due to the interaction of solid particles with the oil/water interface,

369 this effect increases the stability by steric barrier, this is known as a Pickering stabilizer (Yang et

370 al., 2017)

371 In our study the stimulation with CN and CNZ miniemulsions could activate the nitric oxide

372 production in macrophages, indicating their activation. This activation is similar when

373 macrophages are challenge with antigens, adjuvants, or vaccines, inducing nitric oxide production

374 and the capacity to increase the immune response (van den Biggelaar, et al., 2020). The production

375 of nitric oxide induced by the CNZ and CN miniemulsions offers interesting results, since oxygen

376 reactivates intermediates having a great influence on immune responses by activating or inhibiting

377 the action of certain transcription factors or cytokines and by modifying pathways of programmed

378 cell death (Arruda, et al., 2004).

379 The antioxidant total production capacity was studied, determining that both miniemulsions have

380 the capacity to induce higher levels of antioxidants, that can be correlated with the promotion of

381 mitochondrial biogenesis increasing antioxidant enzymes production, decreasing the exacerbation

382 of proinflammatory cytokine response, and blocking or scavenging the excessive response of ROS

383 and RSN, that in higher amounts can affect a healthy immune response (Maldonado, et al., 2021).

384 Is important to mention that cottonseed oil contain antioxidants that can act as exogenous

385   antioxidant sources, however, is possible that antioxidants could be synthesized through different

386   intracellular mechanisms.

387   The results such as leukocyte infiltration after subcutaneous injection and the increase of

388   intraperitoneal cells recruitment, predominantly CD14$^+$ after intraperitoneal miniemulsions

389   injection, similar to the MF59 adjuvant, that is an oil-in-water emulsion containing squalene

390   (4.3%) in citric acid buffer with stabilizing non-ionic surfactants Tween 80 (0.5%) and Span 85

391   (0.5%) used in vaccines (Ko & Kang, 2018). Being the MF59 capable to create an

392   immunocompetent environment at the injection site by recruiting immune cells like neutrophils,

393   macrophages, granulocytes, monocytes, and other immune cells that ingest the antigen (Shah *et*

394   *al.,* 2015). Also, in macrophages the CN and CNZ promotes the phagocytic capacity, similarly to

395   MF59, where antigens and MF59 are phagocyted by neutrophils and monocytes, and later by

396   dendritic cells (DCs) and B cells, then moved to draining lymph nodes (Ko & Kang, 2018). The

397   CN miniemulsion induced the nitric oxide production in mice, likely to FCA where high nitric

398   oxide production is observed (Khan, et al., 2001). Nitric oxide is considered a dual molecule in

399   relation to its benefit on immune system; at low concentration plays a healthy role on immune

400   system but at higher levels immunosuppression is induced (Shreshtha, et al., 2018). This study is

401   not designed to determine the role of nitric oxide, however for the data obtained we assumed that

402   CN or CNZ miniemulsion can activate healthy immune responses.

403   Several studies report that IFN-γ derived from innate immune cells enhances protective

404   antiparasitic Th1 responses and malaria protection after use of adjuvant AS01 (containing two

405   immunostimulants [TLR4 ligand 3-*O*-desacyl-4′-monophosphoryl lipid A (MPL) and the purified

406   saponin QS-21] in a liposome-based formulation) or AS03 (containing α-tocopherol and squalene

407   in an oil-in-water (o/w) emulsion). In addition, the production of IFN-γ could be mediated by IL-

408   2 produced by vaccine-induced effector memory T cells (Burny, et al., 2017). Increase in the IFN-γ

409   and IL-2 production were found in our study with the CN or CNZ miniemulsions treatment.

410   Only CN miniemulsion induced a significant OVA specific IgG production, however no IgG

411   isotype antibodies switch was observed. This can suggest the lack of CD4$^+$ T cell dependency (Ko

412   & Kang, 2018). However, to define these results is necessary the use of CN miniemulsion

413   combined with OVA in CD4$^+$ deficient mice, and to stablish the dependence of Th1 or Th2.

414   The detection of IgG at day 45 can suggest a sustained immunity induced by lymphocyte B and T

415   using CN miniemulsion. The fact of finding a higher IgG concentration induced by FCA than CN

416   miniemulsion can be attributed to the formation of FCA depots at the injection site, inducing

417   delayed germinal center formation promoting higher antibody responses than a non-depot-

418   inducing adjuvant. Such as MF59-like squalene emulsion AddaVax^{TM} after a single

419   immunization (Pedersen, et al., 2020). These results indicate that CN miniemulsion is a non-depot

420   inducing adjuvant.

421   According to our results, we suggest that our miniemulsions have mechanisms of action similar to

422   MF59-like squalene emulsion AddaVax^{TM}. Oils, such as olive, rice bran, corn, peanut, rapeseed,

423   sunflower, and cottonseed contain 0.1 to 4 g/Kg of squalene (He and Corke, 2003; Kalogeropoulos

424   and Andrikopoulos, 2004). Commercial adjuvants such as MF59 and AS03 contain 0.0975 g and

425   0.1069 g per dose, respectively (Shah et al., 2015). If compared commercial squalene adjuvants

426   doses with maximum content in vegetable oils is necessary to use 2.43–2.67 g of oil per dose. This

427   dose is perfectly feasible for farm animals and humans. Vegetable oils can be used in alternative

428   adjuvants to squalene-based emulsion for vaccination, because they contain a long variety of active

429   substances that have effects over immune system (Fox et al., 2011).

430

Conclusions

432   In this study, we synthesized two new miniemulsions cottonseed oil-based, containing or not ZnO

433   nanoparticles with adjuvant and antioxidant capacity, capable of generating leukocyte infiltration

434   and increase cytokines and antibodies production. However, it is necessary to carry out evaluations

435   to determine its effect on the immune system with various antigens and species.

436

Acknowledgements

438   We thank the MsC. Alejandra Arreola Triana for proofreading this article.

439

Funding

441   This research was funded by "Fondo Sectorial de Investigación para la Educación", (grant number

442   A1-S-35951), CONACYT, México. Laboratorio de Inmunología y Virología, Facultad de Ciencias

443   Biológicas from the Universidad Autónoma de Nuevo León.

444

References

446 Arruda MA, Rossi AG, de Freitas MS, Barja-Fidalgo C, Graça-Souza AV. 2004. Heme inhibits
447   human neutrophil apoptosis: Involvement of phosphoinositide 3-kinase, MAPK, and NF-
448   ΚB. *The Journal of Immunology*, *173*: 2023–2030 DOI: 10.4049/jimmunol.173.3.2023

449 Bajaj SD, Tekade PV, Manoja K. 2015. Soxhlet Extraction and FTIR Characterization of Biodiesel
450   from Oil Seeds. International. *Jouranl of Researches in Biosciences Agriculture and*
451   *Technology* 210-216.

452 Burakova Y, Madera R, McVey S, Schlup JR, Shi J. 2018. Adjuvants for animal vaccines. *Viral*
453   *immunology*, *31*, 11-22 DOI: 10.1089/vim.2017.0049

454 Burny W, Callegaro A, Bechtold V, Clement F, Delhaye S, Fissette L, Janssens M, Leroux-Roels
455   G, Marchant A, van den Berg RA, Garçon N, van der Most R, Didierlaurent A M. 2017.
456   Different adjuvants induce common innate pathways that are associated with enhanced
457   adaptive responses against a model antigen in humans. *Frontiers in Immunology* 14: 8-943
458   DOI: 10.3389/fimmu.2017.00943

459 Dardenne M. 2002. Zinc and immune function. *European journal of clinical nutrition 56*: S20-
460   S23 DOI: 10.1038/sj.ejcn.1601479

461 Del Buono D, Luzi F, Tolisano C, Puglia D, Di Michele A. 2022. Synthesis of a lignin/zinc oxide
462   hybrid   nanoparticles   system   and   its   application   by   nano-priming   in
463   Maize. *Nanomaterials 12*: 568 DOI: 10.3390/nano12030568

464 El-Mallah MH, El-Shami SM, Hassanien MMM, Abdel-Razek AG. 2011. Effect of chemical
465   refining steps on the minor and major components of cottonseed oil. *Agriculture and Biology*
466   *Journal of North America 2*: 341-349.

467 Fox CB, Baldwin SL, Duthie MS, Reed SG, Vedvick TS. 2011. Immunomodulatory and physical
468   effects of oil composition in vaccine adjuvant emulsions. *Vaccine* 29: 9563–9572 DOI:
469   10.1016/j.vaccine.2011.08.089

470 Grilo EC, Costa PN, Gurgel CSS, Beserra AFDL, Almeida FNDS, Dimenstein R. 2014. Alpha-
471   tocopherol   and   gamma-tocopherol   concentration   in   vegetable   oils. *Food   Science   and*
472   *Technology 34*: 379-385 DOI: 10.1590/S0101-20612014005000031

473 He HP, Corke H. 2003. Oil and Squalene in Amaranth Grain and Leaf. *Journal of Agricultural*
474   *and Food Chemistry* 51: 7913–7920 DOI: 10.1021/jf030489q

475 Kahn DA, Archer DC, Gold DP, Kelly CJ. 2001. Adjuvant immunotherapy is dependent on
476   inducible nitric oxide synthase. *Journal of Experimental Medicine 193*: 1261–1268 DOI:
477   10.1084/jem.193.11.1261

478 Kalogeropoulos N, Andrikopoulos, NK. 2004. Squalene in oils and fats from domestic and
479   commercial fryings of potatoes. *International journal of food sciences and nutrition* 55: 125-
480   129 DOI: 10.1080/09637480410001666531

481 Ko EJ, Kang SM. 2018. Immunology and efficacy of mf59-adjuvanted vaccines. *Human Vaccines*
482   *& Immunotherapeutics 14*: 3041–3045 DOI: 10.1080/21645515.2018.1495301

483 Lee GY, Han SN. 2018. The role of vitamin E in immunity. *Nutrients 10*: 1614 DOI:
484   10.3390/nu10111614

485 Lucarini M, Zuorro A, Di Lena G, Lavecchia R, Durazzo A, Benedetti B, Lombardi-Boccia G.
486   2020. Sustainable management of secondary raw materials from the Marine Food-Chain: A
487   case-study perspective. *Sustainability 12*: 8997 DOI: 10.3390/su12218997

488 Maldonado E, Rojas DA, Urbina F, Solari A. 2021. The use of antioxidants as potential co-
489   adjuvants   to   treat   chronic   chagas   disease. *Antioxidants 10*:   1022   DOI:
490   10.3390/antiox10071022

491 Malik P, Ameta RK, Singh M. 2016. Physicochemical study of curcumin in oil driven
492   nanoemulsions with surfactants. *Journal of Molecular Liquids 220*: 604–622 DOI:
493   10.1016/j.molliq.2016.04.126

494 Nagaraju G, Prashanth SA, Shastri M, Yathish KV, Anupama C, Rangappa D. 2017.
495   Electrochemical heavy metal detection, photocatalytic, photoluminescence, biodiesel
496   production and antibacterial activities of Ag–ZnO nanomaterial. *Materials Research*
497   *Bulletin 94*: 54-63. DOI: 10.1016/j.materresbull.2017.05.043

498 Pedersen GK, Wørzner K, Andersen P, Christensen D. 2020. Vaccine adjuvants differentially
499   affect kinetics of antibody and germinal center responses. *Frontiers in Immunology 11*. DOI:
500   10.3389/fimmu.2020.579761

501 Shah RR, Brito LA, O'Hagan DT, Amiji MM. 2015. Emulsions as Vaccine Adjuvants. In: Foged
502   C, Rades T, Perrie Y, Hook S. Subunit Vaccine Delivery. Advances in Delivery Science and
503   Technology. Springer, New York, NY DOI: 10.1007/978-1-4939-1417-3_4

504 Shah SN, Ali SI, Ali SR, Naeem M, Bibi Y, Ali SR, Raza SM, Khan Y, Sherwani SK. 2016.
505   Synthesis   and   Characterization   of   Zinc   Oxide   Nanoparticles   for   Antibacterial

506 Applications. *Journal of Basic and Applied Sciences 12*: 205–210 DOI: 10.6000/1927-
507 5129.2016.12.31

508 Shah SN, Mahesar SA, Abro KA, Sherazi STH, Nizamani SM. 2017. FTIR characterization and
509 physicochemical evaluation of cottonseed oil. *Pakistan Journal of Analytical &*
510 *Environmental Chemistry*, *18*: 46-53. DOI: 10.21743/pjaec/2017.06.04

511 Shahbazi S, Bolhassani A. 2016. Immunostimulants: types and functions. *Journal of Medical*
512 *Microbiology and Infectious Diseases 4*: 45-51.

513 Shreshtha S, Sharma P, Kumar P, Sharma R, Singh SP. 2018. Nitric oxide: It's role in
514 immunity. *Journal of Clinical and Diagnostic Research* DOI:
515 10.7860/jcdr/2018/31817.11764

516 Thommen Maciel Sartor I, Moleta Colodel E, Albuquerque D. 2011. Adjuvant activity of rice oil
517 on the immune response to ovalbumin. *Vaccimonitor* 20: 1-5

518 Van den Biggelaar R, van Eden W, Rutten V, Jansen C. 2020. Nitric oxide production and Fc
519 receptor-mediated phagocytosis as functional readouts of macrophage activity upon
520 stimulation with inactivated poultry vaccines in vitro. *Vaccines 8*: 332 DOI:
521 10.3390/vaccines8020332

522 Vasile OR, Serdaru I, Andronescu E, Truşcă R, Surdu VA, Oprea O, Ilie A, Vasile BS. 2015.
523 Influence of the size and the morphology of zno nanoparticles on cell viability. *Comptes*
524 *Rendus Chimie* 18: 1335–1343 DOI: 10.1016/j.crci.2015.08.005

525 Xin X, Zhang H, Xu G, Tan Y, Zhang J, Lu X. 2013. Influence of CTAB and SDS on the properties
526 of oil-in-water nano-emulsion with paraffin and span 20/Tween 20. *Colloids and surfaces*
527 *A: physicochemical and engineering aspects*, *418*: 60-67. DOI:
528 10.1016/j.colsurfa.2012.10.065

529 Yang Y, Fang Z, Chen X, Zhang W, Xie Y, Chen Y, Yuan W. 2017. An overview of Pickering
530 emulsions: solid-particle materials, classification, morphology, and applications. *Frontiers*
531 *in pharmacology 8*: 287. DOI: 10.3389/fphar.2017.00287

DLS analysis of the miniemulsions CN and CNZ at 25°C.

Miniemulsions	Time(months)		
	0	1	3
CN			
Droplet size (d.nm)	543.1	506.1	542.7
PDI	0.074	0.192	0.225
Zeta Potential (mV)	-26.6	-22.1	-13
CNZ			
Droplet size (d.nm)	320	266.1	259.6
PDI	0.449	0.279	0.312
Zeta Potential (mV)	-28.1	-30.6	-29.5

Functional groups of cottonseed oil, α-tocopherol, and miniemulsion CN and CNZ.

FT-IR spectrum of miniemulsions	
Functional group	**Wavenumber (cm^{-1})**
Cottonseed oil	
C-H	2922
COOH	2856
C=O	1744
C-H	1465
C-O	1156
α- Tocopherol	
CH$_2$	2927
CH$_3$	2867
C=C	1758
C$_6$H$_5$	1461
CH$_3$	1365
CH$_2$	1203
CN	
Interaction with the group COOH (cottonseed oil)	2856
Interaction with the group C=O (Cottonseed oil)	1745
Interaction with the group C-O (Cottonseed oil)	1156
Interaction with the group C=C (α- Tocopherol)	1758
Interaction with the group C$_6$H$_5$ (α- Tocopherol)	1461
CNZ	
Interaction with the group COOH (cottonseed oil)	2856
Interaction with the group C=C (α- Tocopherol)	1758
Interaction with the group C=O (Cottonseed oil)	1745
Interaction with the group C$_6$H$_5$ (α- Tocopherol)	1461
Interaction with the group C-O (Cottonseed oil)	1156
Nanoparticles of ZnO	670

Figure 1

Particle size distribution measurement and AFM images of miniemulsions.

(**A**) Measurements of (**1**) CN and (**2**) CNZ by dynamic light scattering. (**B**) Measurements of zeta potential of (**1**) CN and (**2**) CNZ by dynamic light scattering. (**C**) Images by AFM 2D of (**1**) CN and (**3**) CNZ, and 3D of (**2**) CN and (**4**) CNZ
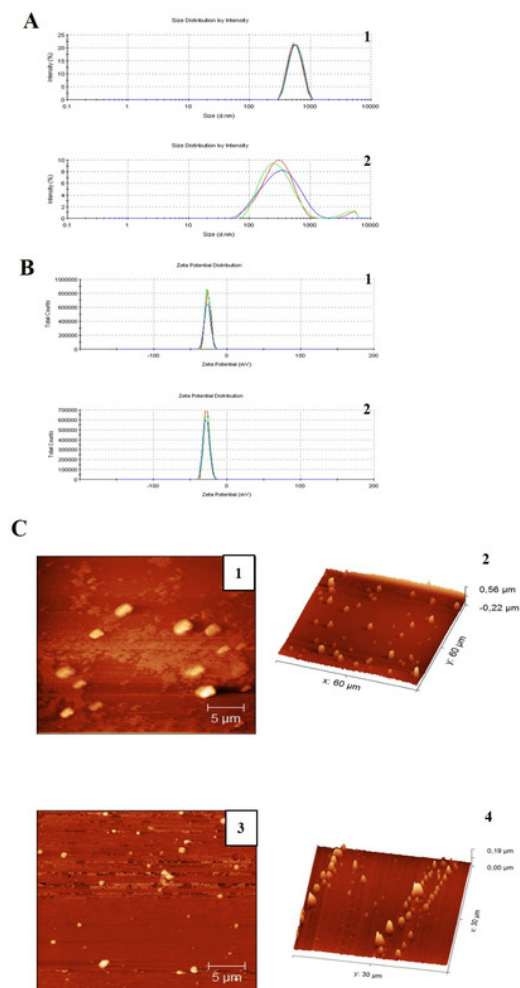
Figure 2

Figure 2. Characterization of zinc oxide nanoparticles synthesized

(A) FTIR spectra of zinc sulfate (precursor). (**B**) FTIR spectra ZnO nanoparticles. (**C**) Scanning electron microscopy (SEM) image of the synthesized zinc oxide nanoparticles. (**D**) The X-ray diffraction picks observed correlated with JCPDS card No 01-089- 0510 indicates the hexagonal phase of ZnO.
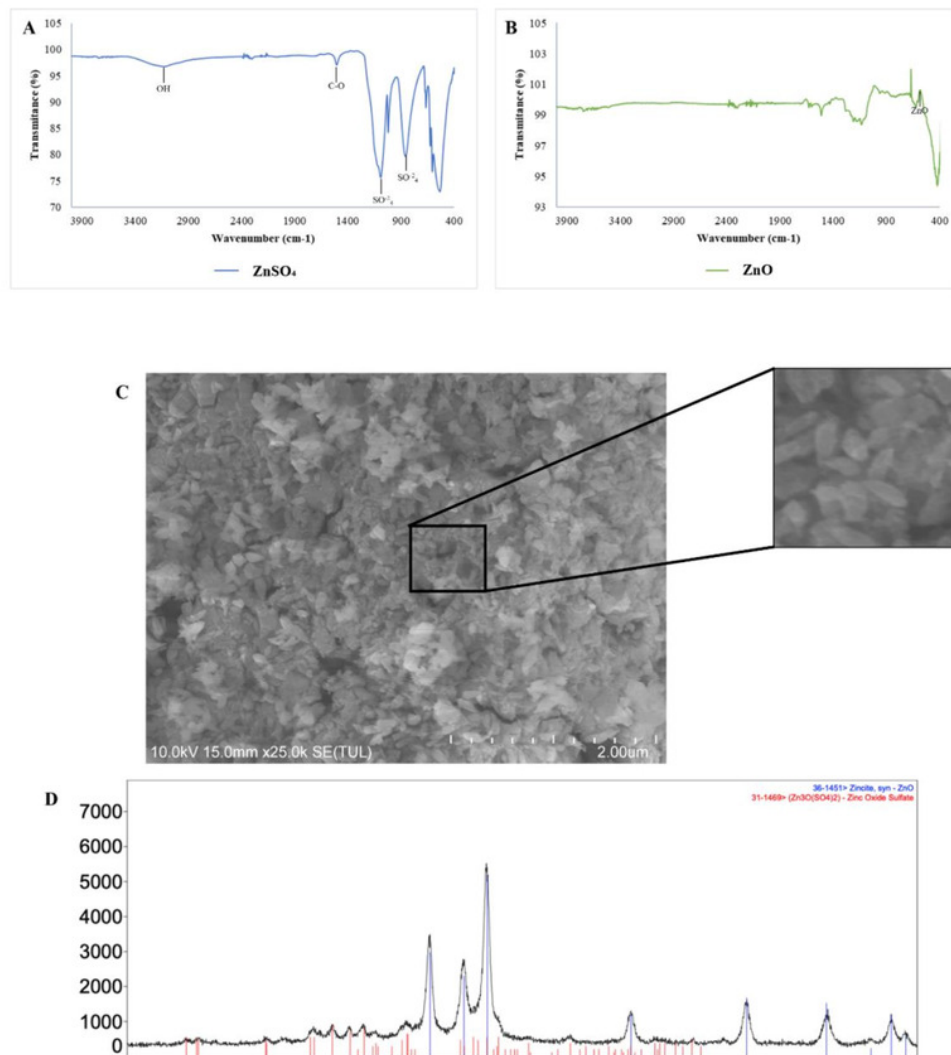
Figure 3

Characterization of miniemulsion CN and CNZ.

(**A**) FTIR spectra of cottonseed oil, (**B**) FTIR spectra of α-tocopherol, (**C**) FTIR spectra of CN,

(**D**) FTIR spectra of CNZ and (**E**) FTIR spectra of miniemulsions CN, CNZ, and cottonseed oil.
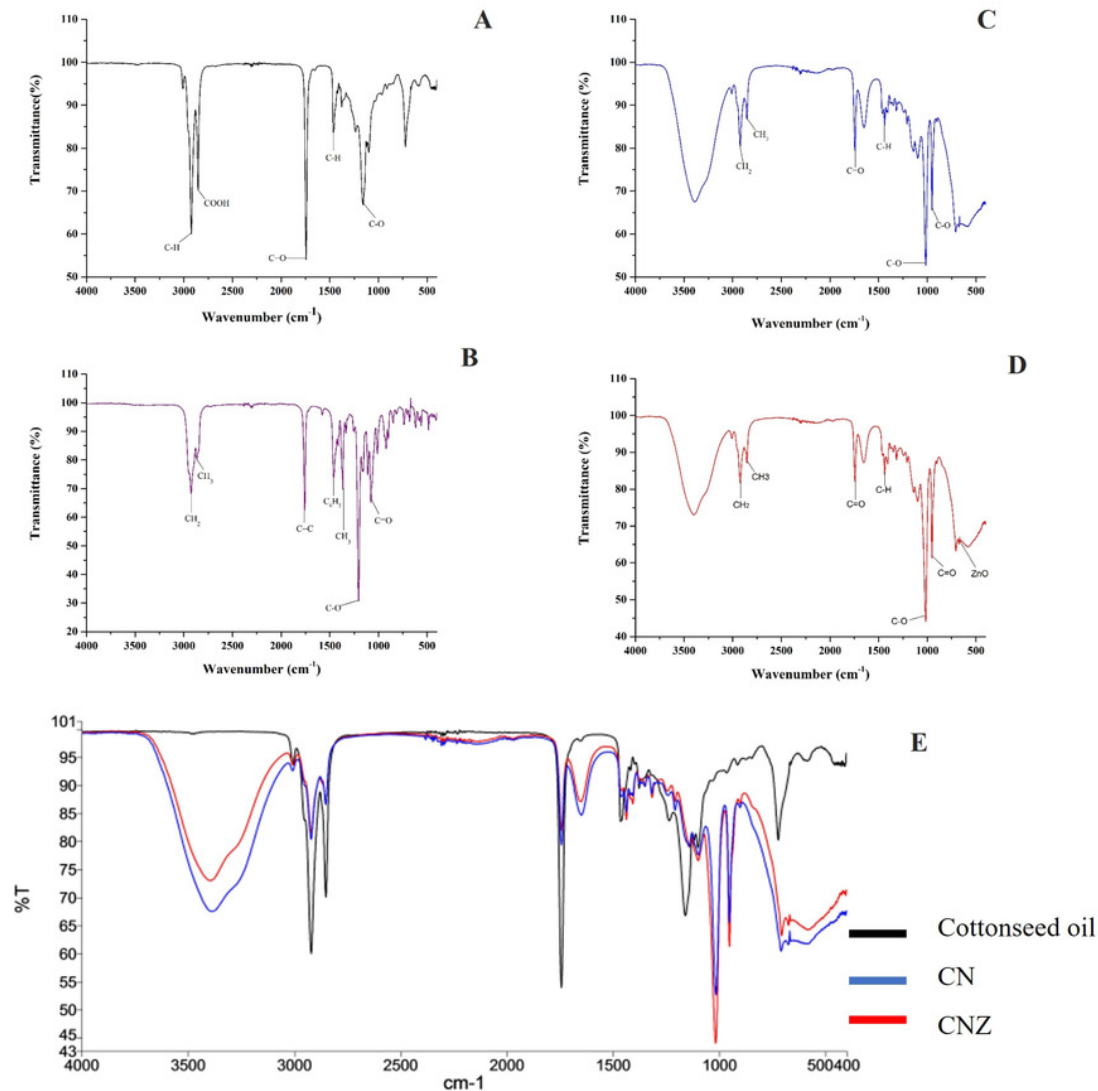
Figure 4

Effect of the miniemulsions on cell viability.

The miniemulsions (CN and CNZ) at concentrations of 1.25 to 10 µL/mL did not affect the viability of macrophages, splenocytes and thymocytes (2×10^5 cells/well with 3 replicates) evaluated by MTT. Values are expressed as mean ± SE. The analysis was performed by means of an ANOVA test with a significance of $P < 0.05$.
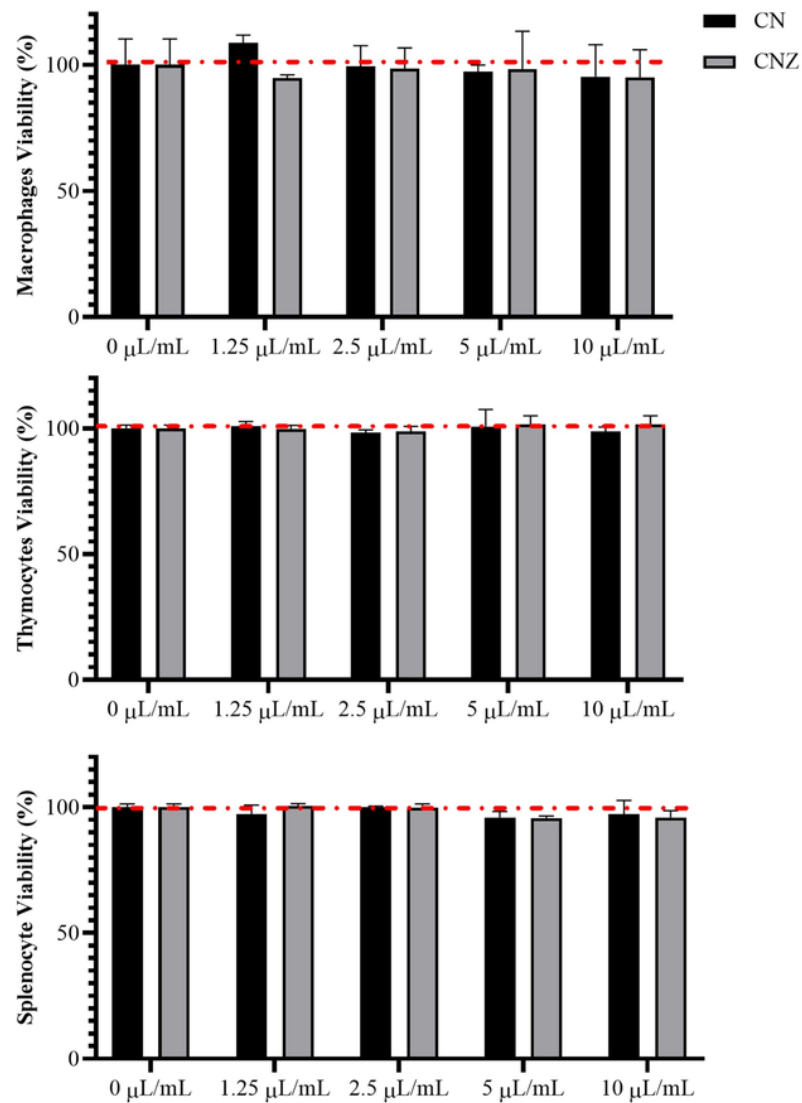
Figure 5

Production of RNS in murine peritoneal macrophages.

Murine peritoneal macrophages (2×10^5 cells/well with 3 replicates) were stimulated with different miniemulsions (CN and CNZ) doses. LPS 5 µg/mL was used as control (+) and cells without treatment as Control (-). The RNS were determinate as nitrite. An ANOVA ($p < 0.05$) was performed to compare the effect of the different doses. To determine the difference between treatments, a comparison of means was performed by Tukey.
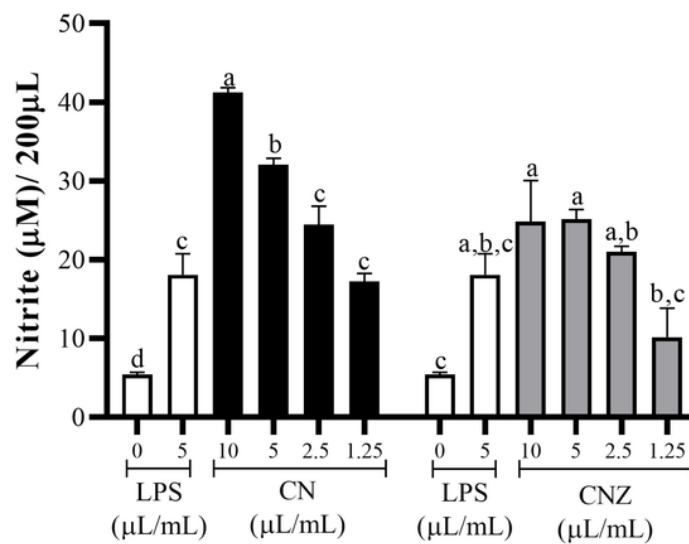
Figure 6

Total antioxidant capacity (TAC) in murine peritoneal macrophages.

Murine peritoneal macrophages (2×10^5 cells/well with 3 replicates) stimulated with different doses of miniemulsions (CN and CNZ). LPS 5 µg/ml was used as control (+) and cells without treatment as Control (-). An ANOVA ($p < 0.05$) was performed to compare the effect of the different doses. To determine the difference between treatments, a comparison of means was performed by Tukey.
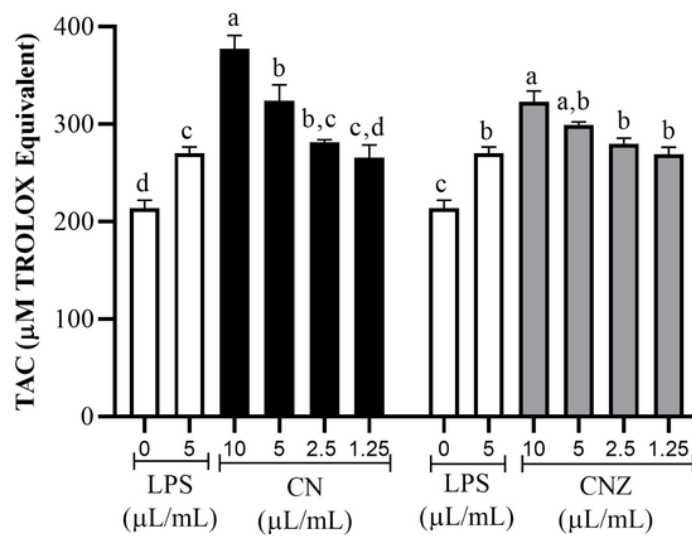
Figure 7

Leukocytes migration to the inoculation site of the miniemulsions.

H&E-stained histological images at 40X of the s.c. inoculation site. of treatments a) Control without adjuvant, b) ACF, c) CN and d) CNZ using Ovalbumin as antigen. Inflammation and leukocyte infiltration (black arrow) are observed in treatments b) ACF, c) CN and d) CNZ.
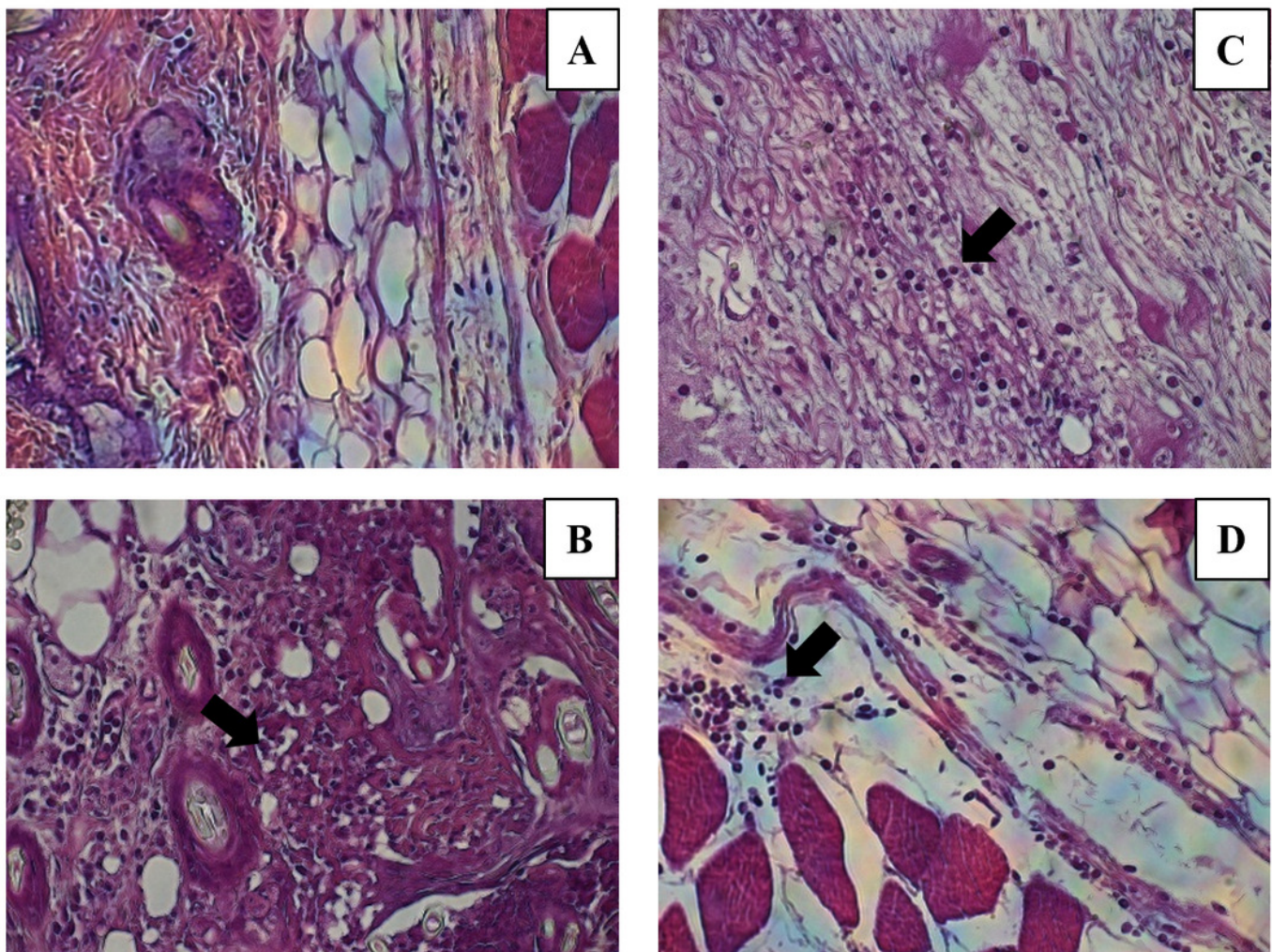
Figure 8

Quantification of macrophages recruited to the inoculation site.

Intraperitoneal macrophages (n= 12 mices, 3 per tratment) recruited were determinate by flow cytometry. (**A**) Gate selection (macrophage population) by size and granularity, and reading by the FL1 channel of the CD14$^+$ receptor. (**B**) Estimation of the amount (macrophages/μL) by size and granularity in murine peritoneal macrophages stimulated *in situ (*in peritoneum). (**C**) CD14$^+$ expression in murine peritoneal macrophages stimulated *in situ* for 24 h. All statistical analysis were performed by means of an ANOVA, determining differences (p<0.05) by means of a Tukey analysis.
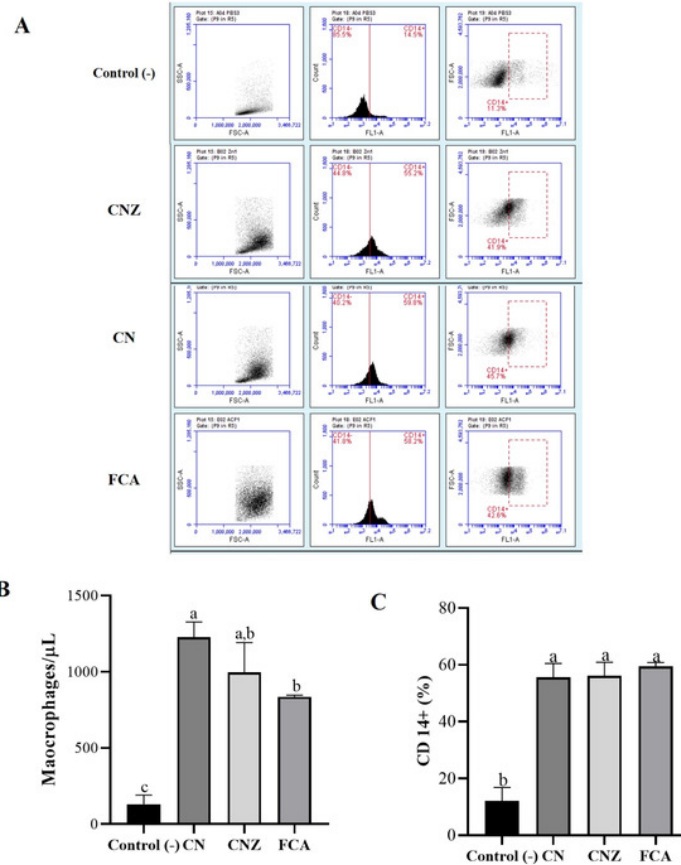
Figure 9

Uptake activity of macrophages stimulated with the miniemulsions.

Macrophages (2×10^5 cells/well with 7 replicates) were stimulate with the miniemulsions CN, CNZ or negative control for 2 h. Disodium clodronate (0.6 mg/mL) was used as non-

phagocytic (Control -) (2×10^5 cells/well with 4 replicates). An ANOVA ($p < 0.05$) was

performed to compare the effect of the different treatments. To determine the difference

between treatments, a comparison of means was made by Tukey.
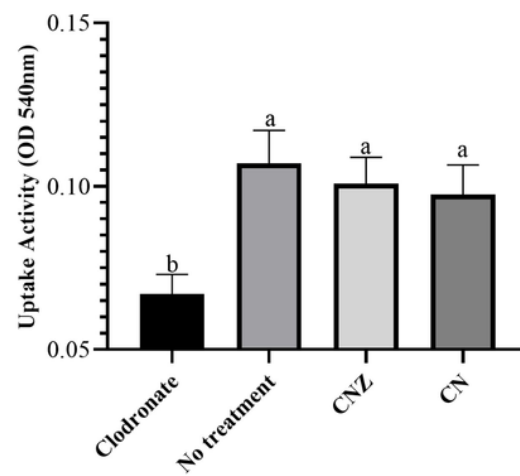
Figure 10

Qualitative evaluation of macrophage phagocytic activity.

The phagocytic activity was evaluated by means of 100X fluorescence microscopy in macrophages treated with a) Clodronate disodium (0.6 mg/mL) as (Control -) of no phagocytosis, b) without treatment, c) CN (10μL/mL) and d) CNZ (10μL/mL).
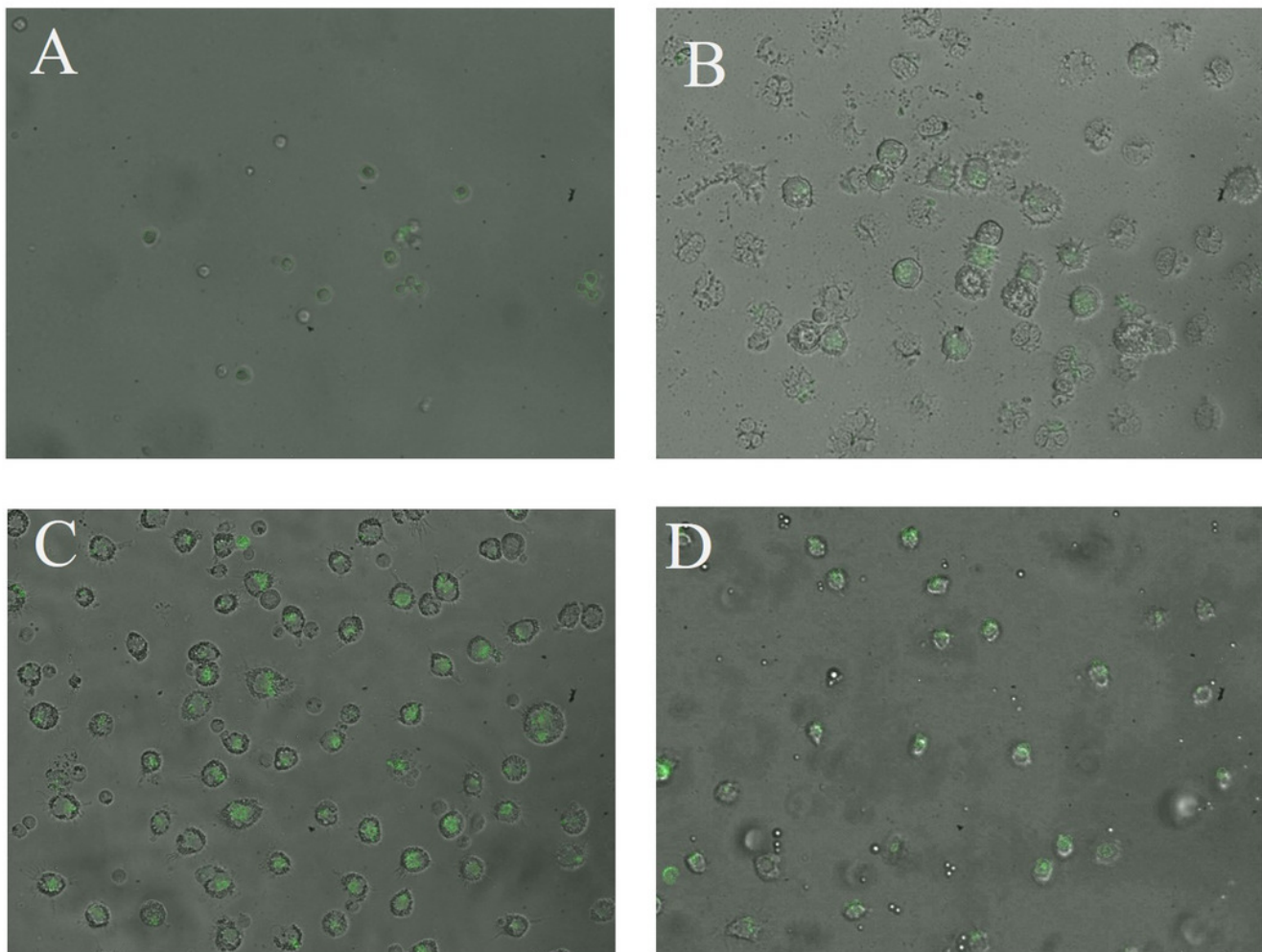
Figure 11

Phagocytic activity of macrophages co-cultured with *C. albicans*

The co-cultured (n= 24) macrophages (1X10^6 cells) / *C. albicans* (1X10^6-1X10^8 cells) were treated with miniemulsions (CN or CNZ) at 4 times. (**A**) Residual colony forming units (CFU) after different times in co-culture. (**B**) production of nitrite oxide (NO) measured in the form of nitrite induced by the co-cultivation. The values are expressed as the mean (± SE). An ANOVA (p < 0.05) was performed to compare the effect of the different doses. To determine the difference between treatments, a comparison of means was made by Tukey.
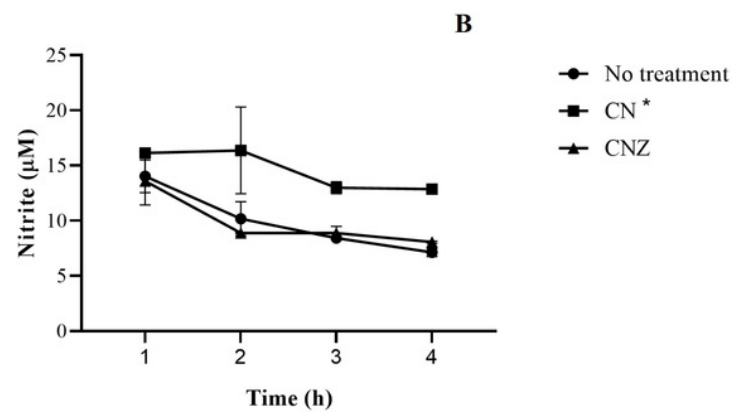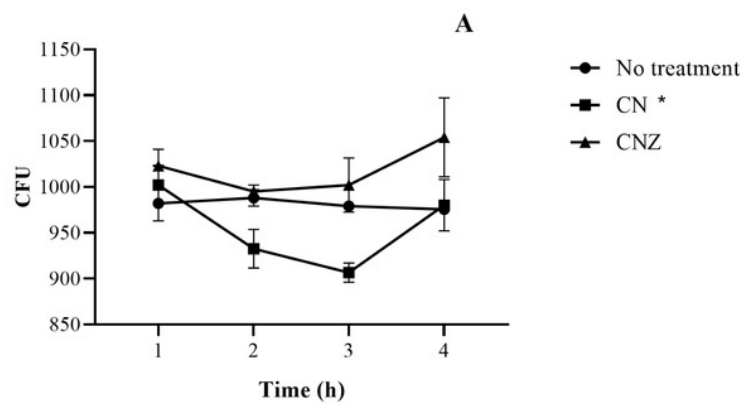
Figure 12

Effect of miniemulsions on cytokine production in a murine model.

Serum levels (Pg/ mL) of cytokines (INFγ, IL2 and IL 10) in BALB/c mice (n= 30) inoculated s.c. with 50 µl of miniemulsions (CN and CNZ), positive control FCA or negative control an antigen (ovalbumin without adjuvant) on days 0 and 14 of the protocol. At 7, 14 and 28 days after the first inoculation. Ovalbumin (OVA) was used as antigen in all treatments. Values are expressed as mean ± SE. When a difference was observed (p> 0.05), a Tukey test was performed to determine differences.
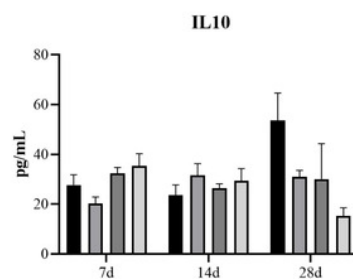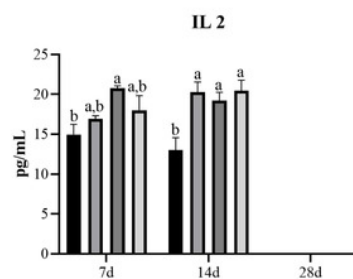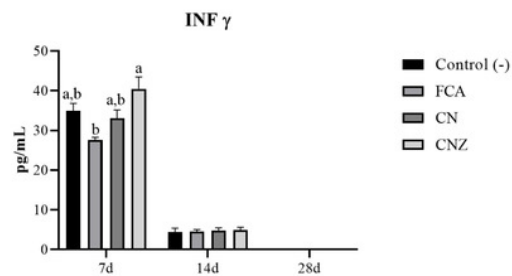
Figure 13

Effect of miniemulsions on antibody isotypes production in a murine model.

Antibody isotypes (IgG1, IgG2a, IgG2b, IgG3, IgA and IgM Serum levels) in BALB/c mice (n= 30) inoculated s.c. with 50 µl of miniemulsions (CN and CNZ), positive control (FCA) or negative control (ovalbumin without adjuvant) on days 0 and 14 of the protocol. Ovalbumin (OVA) was used as antigen in all treatments. Values are expressed as mean ± SE. When a difference was observed (p> 0.05), a Tukey test was performed to determine differences.
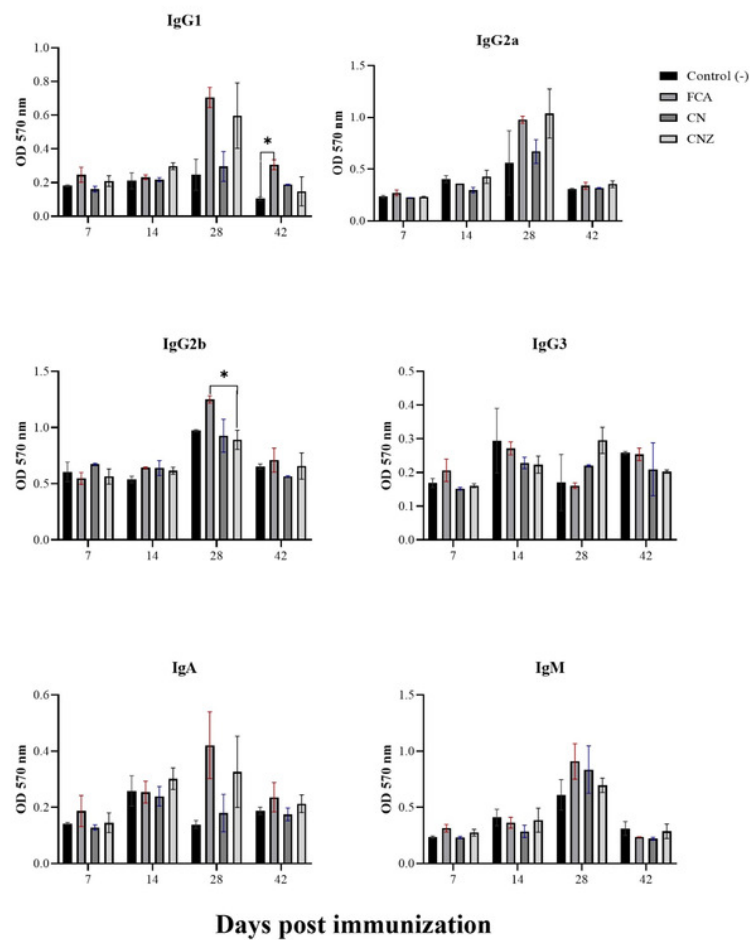
Figure 14

Effect of miniemulsions on specific antibodies production in a murine model.

Specific antibodies against OVA (IgG) 45 days after the last immunization (antigen + adjuvant). Mice (n= 30) were challenged with the antigen (OVA) on day 42 post vaccination. Values are expressed as mean ± SE. When a difference was observed (p> 0.05), a Tukey test was performed to determine differences.